Enhanced Seebeck coefficient in EuTe/PbTe [100] short-period superlattices

Akihiro Ishida,[1,a)] Daoshe Cao,[1] Sinsuke Morioka,[1] Martin Veis,[1] Yoku Inoue,[1] and Takuji Kita[2]
[1]*Department of Electrical and Electronic Engineering, Shizuoka University, Johoku 3-5-1, Hamamatsu 432-8561, Japan*
[2]*TOYOTA Motor Co., Mijyuku 1200, Susono 410-1193, Japan*

(Received 5 March 2008; accepted 3 April 2008; published online 9 May 2008)

Theoretical and experimental studies on Seebeck effect in EuTe/PbTe superlattices were performed. Theoretical calculations, which take into account temperature dependent band gap, nonparabolicity, and anisotropy of effective masses in the PbTe conduction band, were performed in the framework of Boltzmann equation in which enhancement of Seebeck coefficient in EuTe/PbTe short-period superlattices grown in [100] direction was predicted. The EuTe/PbTe short-period superlattices with few monolayers EuTe were prepared on KCl (100) substrate and an enhanced Seebeck coefficient was observed in these superlattices as expected by theoretical calculations. © *2008 American Institute of Physics*. [DOI: 10.1063/1.2917482]

In low dimensional structure, an enhancement of the thermoelectric figure of merit $ZT=\sigma S^2T/\kappa$, where σ is electrical conductivity, S is Seebeck coefficient, and κ is thermal conductivity, was predicted and has been systematically studied.[1–9] The enhancement of ZT has been achieved through the increase in Seebeck coefficient and decrease in thermal conductivity. The decrease in thermal conductivity by multiple-layer structure or quantum dot structure has been reported and the enhancement of the ZT has been mainly obtained through this effect.[3–5] Hicks *et al.* reported the enhancement of Seebeck coefficient in PbEuTe/PbTe superlattice system,[2] and Harman *et al.* reported enhancement of Seebeck coefficient in PbTe/PbTeSe quantum dot structure.[3] The Seebeck effect in two-dimensional system is often discussed in terms of carrier concentration inside the quantum wells.[2,7] However, discussion of the Seebeck effect in terms of carrier concentration averaged over the superlattice (SL) volume is more realistic because the step height of the density of states depends on the SL period and the electrical conductivity σ is also directly related to the averaged carrier concentration. High and steep density of states (DOS) is effective in increasing the Seebeck coefficient, while SL structure with very thin barrier layer is effective in increasing the step height of the DOS. However, thin potential barrier broadens the quantum subband, resulting in a moderate step in the DOS. Short-period SLs combined with narrow-gap and wide-gap semiconductors are useful to obtain steep density of states with large step height. In this letter, we describe theoretical and experimental Seebeck coefficients of PbTe based SLs and show that EuTe/PbTe [100] short-period SLs with few monolyers of EuTe are useful to obtain enhanced Seebeck coefficient.

Figures 1(a)–1(c) show the DOS of PbEuTe/PbTe (10 nm/10 nm) [111], EuTe/PbTe (0.75 nm/5 nm) [111], and EuTe/PbTe (0.66 nm/5 nm) [100] SLs. Carrier distribution $n(E)$ in the SL and DOS in bulk PbTe are also shown in these figures. Since PbTe has conduction band minima and valence band maxima at L points of Brillouin zone with large effective-mass anisotropies ($m_l/m_t \approx 10$), two kinds of quantum states are formed by longitudinal valley along the SL direction (denoted by 1_l, 2_l, etc.) and three equivalent valleys oblique to the SL direction (denoted by 1_o, 2_o).[10] Total step height of the two-dimensional density of states for all oblique valleys is one order higher than that of the longitudinal valley because the DOS effective mass of the oblique valley is three times larger than that of the longitudinal valley. The step heights of the two-dimensional densities of states in the SL increase with the decrease in the SL period. Thus, high steplike density of states is obtained in the short-period SL. In [100] SL, all valleys have the same angle to the SL direction and the subband structure becomes simple with high step in the density of states, as shown in the Fig. 1(c). Kane-type nonparabolicity $\Sigma\ \hbar^2k_ik_j/2m_{ij}=E(1+E/E_g)$ was assumed in the calculation,[10] and the two-dimensional density of states increases proportionally to $(1+2E/E_g)$. Figure 2 shows a schematic band structure for the explanation of Seebeck effect in PbTe based SL. Energy band gap of PbTe strongly increases with the temperature and effective masses of electrons proportionally increase to the band gap.[11] Seebeck coefficient of the material is given by $S=(1/e)dE_F/dT=-(1/e)d(E_C-E_F)/dT+(1/e)dE_C/dT$, where the E_C-E_F is a function of density of states and the dE_C/dT is determined by the balance between the thermal-diffusion current and drift current. In the IV-VI semiconductor SL, dE_C/dT is also affected by the temperature dependence of

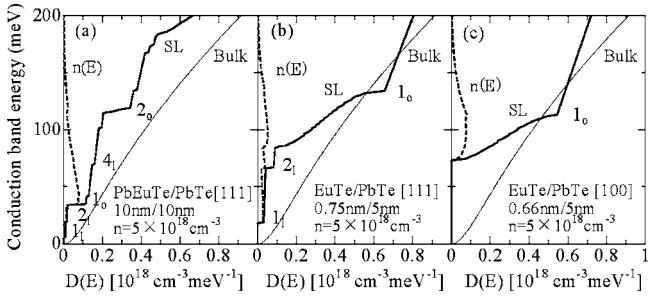

FIG. 1. Densities of states in (a) PbEuTe/PbTe (10 nm/10 nm) [111] superlattice, (b) EuTe/PbTe (0.75 nm/5 nm) [111] short-period superlattice and (c) EuTe/PbTe (0.66 nm/5 nm) [100] short-period superlattice compared to bulk density of states. Carrier distribution is also shown by a dashed line in each figure.

a)Electronic mail: tdaishi@ipc.shizuoka.ac.jp.

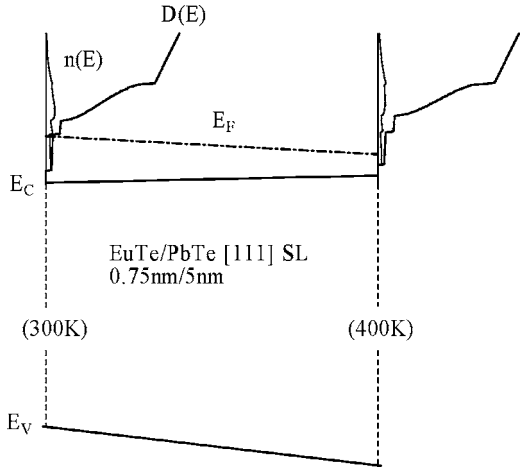

FIG. 2. Schematic band structure for the explanation of Seebeck effect of PbTe based SL. Energy band gap of PbTe increases with temperature.

quantum levels due to temperature dependent effective masses.[11] The drift current density J_{drift} and thermal-diffusion current density J_{thermal} are derived from the Bolzmann equation, and given as

$$J_{\text{drift}} = \left(\frac{e^2}{4\pi^3 kT}\right)\sum_{V,m}\left(\frac{1}{e}\frac{dE_C}{dx} + \frac{1}{e}\frac{dE_{zVm}}{dx}\right)\int \tau v_x^2 f_0(1-f_0)d^3k, \tag{1}$$

$$J_{\text{thermal}} = \left(\frac{e}{4\pi^3 kT}\right)\frac{dT}{dx}\sum_{V,m}\int \tau v_x^2 f_0(1-f_0)\left[\frac{E-E_F}{T} - \frac{d(E_C-E_F)}{dT}\right]d^3k. \tag{2}$$

Here, in-plane temperature gradient is taken in the x direction, τ is the relaxation time of carriers, v_x is the electron velocity along the x direction, E_{zVm} is the quantum level of mth subband in Vth valley, and the summation is taken over all subbands in all L-point valleys. We replaced electric field E_x in conventional Boltzmann equation to $(1/e)d(E_C+E_{zVm})/dx$, considering that the drift current comes from the real-space gradient of quantum levels. Seebeck coefficient is given by the balance between the drift and thermal-diffusion currents and calculated by

$$S = -\frac{1}{e}\frac{d(E_C-E_F)}{dT} - \frac{1}{e}\frac{\sum_{V,m}\int \tau v_x^2 f_0(1-f_0)\left[\frac{dE_{zVm}}{dT} + \frac{E-E_F}{T} - \frac{d(E_C-E_F)}{dT}\right]d^3k}{\sum_{V,m}\int \tau v_x^2 f_0(1-f_0)d^3k}. \tag{3}$$

This equation can be used also for bulk materials if dE_{zVm}/dT term is removed and the summation is taken only for four three-dimensional ⟨111⟩ valleys. In the PbTe based SLs, the value dE_{zVm}/dT becomes negative owing to the increase in effective masses with temperature, resulting in a small thermal-diffusion current or a decrease in $-dE_C/dT$. On the other hand, the effective-mass variation increases the $d(E_C-E_F)/dT$ in the first term in Eq. (3). In the previous papers, the temperature dependence has never been considered, although it strongly affects the Seebeck coefficient. In the Kane-type band structure, band edge effective masses are proportional to the band gap and effective masses at energy E measured from the band edge proportionally increase to $(1+2E/E_g)$. This effective-mass variation can explain interband-absorption properties of IV–VI based SLs.[10] Next, we describe the effect of growth direction on the Seebeck coefficient. In the EuTe/PbTe [111] SL, bound quantum state in the longitudinal valley is considerably lower than that of oblique valley, resulting in relatively high electron concentration in the longitudinal valley. The ratio of electron concentration in the oblique valley compared to the longitudinal valley increases at high temperature, which results in a decrease in the average electron velocity along the x direction. Thus, the value $-dEc/dT$ of the [111] SL becomes smaller than that of the [100] SL, which results in a small Seebeck coefficient of the [111] SL compared to the [100] SL. Figure 3 shows theoretical dependence of Seebeck coefficients on the carrier concentration for PbEuTe/PbTe (10 nm/10 nm) [111] SL, PbEuTe/PbTe (10 nm/10 nm) [100] SL, EuTe/PbTe (0.75 nm/5 nm) [111] SL, EuTe/PbTe(0.66 nm/5 nm) [100] SL, and bulk PbTe. Band gap of the PbEuTe was assumed to be 660 meV with the conduction band offset of 170 meV. The conduction band offset of the EuTe/PbTe heterojunction was assumed to be 1000 meV with the parameter used in Refs. 10 and 12. En-

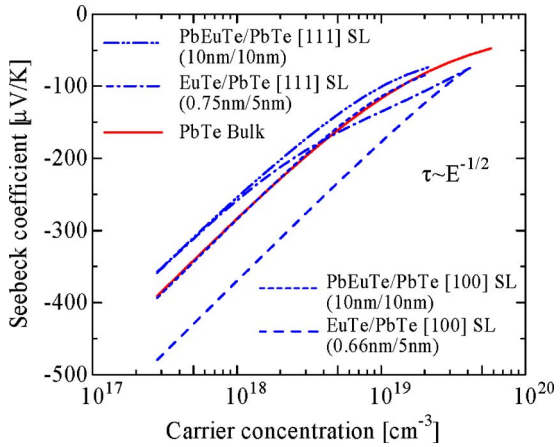

FIG. 3. (Color online) Theoretical Seebeck coefficient of PbTe films, PbEuTe/PbTe (10 nm/10 nm) [111] SLs, PbEuTe/PbTe (10 nm/10 nm) [100] SLs, EuTe/PbTe (0.75 nm/5 nm) [111] SLs, and EuTe/PbTe (0.66 nm/5 nm) [100] SLs calculated from Eq. (3). Considerable enhancement of Seebeck effect in the EuTe/PbTe [100] SLs is expected.

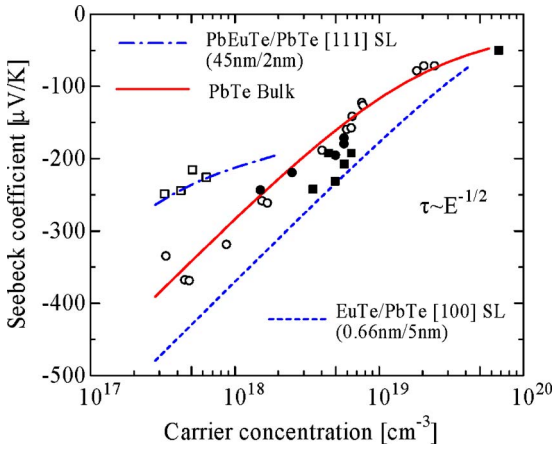

FIG. 4. (Color online) Comparison between theoretical and experimental Seebeck coefficients for PbTe films [○: work of Beyer *et al.* (Ref. 14), ●: this work], PbEuTe/PbTe (45 nm/2 nm) [111] SLs [□: work of Hicks *et al.* (Ref. 2)], and EuTe/PbTe (0.66 nm/5 nm) [100] SLs (□: this work). Good agreement between theoretical and experimental Seebeck coefficients was obtained and significant increase in Seebeck coefficients compared to PbTe films was obtained in the EuTe/PbTe (0.66 nm/5 nm) [100] SLs.

ergy dependent relaxation time $\tau \propto E^{-1/2}$ was used for the calculation assuming dominant acoustic-phonon scattering. Theoretical Seebeck coefficients of [100] SLs are higher than those of [111] superlattices as predicted by Casian *et al.*[8] and considerably high Seebeck coefficient is expected in the EuTe/PbTe (0.66 nm/5 nm) [100] SL.

EuTe/PbTe short-period SLs with 5 nm PbTe and 1–2 ML EuTe were prepared by hot wall epitaxy on KCl (100) substrates by using PbTe, Eu, and Te as source materials.[12] Substrate temperature during growth was 280 °C and total thicknesses of the SLs were 1.5–4 μm. The film thickness was calculated from the optical transmission spectrum measured by Fourier transform infrared spectroscopy. Carrier concentration was obtained from Hall measurement by using the equation $R_H = -\gamma/en$. In simple model for nondegenerate semiconductors, γ becomes 1.18 under predominant phonon scattering. Real γ depends also on effective-mass anisotropy, carrier concentration, and nonparabolicity. The anisotropy decreases the value about 20% under low magnetic field.[13] Thus, $\gamma = 1$ was assumed as conventionally adopted within the error of 20%. Seebeck coefficient was measured with ZEM-2 (ULVAC-Riko). The measurement was performed in a helium atmosphere to decrease the temperature error. Temperature difference between two thermocouples was applied in 5 K. Seebeck coefficient was measured within the error of 10%. Figure 4 shows Seebeck coefficients of PbTe films (○: work of Beyer *et al.*,[14] ●: this work), EuTe/PbTe [100] short-period SLs (■: this work), and PbEuTe/PbTe (45 nm/2 nm) SLs (□: work of Hicks *et al.*[2]), compared to the theoretical dependence calculated from Eq. (3). The carrier concentration in the horizontal axis is the averaged value over the superlattice structure. The PbEuTe/PbTe (45–2 nm) SL with a carrier concentration of 1×10^{19} cm^{-3} inside the well has the averaged carrier concentration around 4×10^{17} cm^{-3}. Since overflow carriers into the PbEuTe barrier layer are significant in the PbEuTe/PbTe (45 nm/2 nm) SL, two kind of relaxation times were assumed: Relaxation time of electrons in the quantum states with $E_{zVm} > \Delta E_C$ was taken to be one-fifth of the relaxation time of the electrons in the quantum well, taking into account the electron mobility difference between the SL and PbEuTe film. No modification was done for the relaxation time in PbTe film and EuTe/PbTe superlattices, only assuming $\tau \propto E^{-1/2}$. Excellent agreement between experimental and theoretical Seebeck coefficients were obtained, indicating considerably high Seebeck coefficient in the EuTe/PbTe short-period SLs compared with PbTe films and PbEuTe/PbTe SLs.

In summary, theoretical calculation, which takes into account nonparabolicity and anisotropy of effective masses, temperature dependence of band gap, and effective masses in the PbTe conduction band, predicted enhanced Seebeck effect in the EuTe/PbTe [100] short-period superlattices. PbTe films and EuTe/PbTe short-period superlattices were prepared on KCl (100) by hot wall epitaxy and experimental Seebeck effect was compared to the theoretical calculation. Excellent agreement between the experimental and theoretical data was obtained, indicating considerably high Seebeck coefficient in EuTe/PbTe short-period SLs compared to PbTe films and PbEuTe/PbTe SLs.

[1] L. D. Hicks and M. S. Dresselhaus, Phys. Rev. B **47**, 12727 (1993).
[2] L. D. Hicks, T. C. Harman, X. Sun, and M. S. Dresselhaus, Phys. Rev. B **53**, R10493 (1996).
[3] T. C. Harman, P. J. Taylor, D. L. Spears, and M. P. Walsh, J. Electron. Mater. **29**, L1 (2000).
[4] H. Beyer, J. Nurnus, H. Böttner, and A. Lambrecht, Appl. Phys. Lett. **80**, 1216 (2002).
[5] J. C. Caylor, K. Coonley, J. Stuart, T. Colpitts, and R. Ventasubramanian, Appl. Phys. Lett. **87**, 023105 (2005).
[6] R. Venkatasubramanian, E. Siivoka, T. Colpitts, and B. O'Quinn, Nature (London) **413**, 597 (2001).
[7] T. Koga, T. C. Harman, S. B. Cronin, and M. S. Dresselhaus, Phys. Rev. B **60**, 14286 (1999).
[8] A. Casian, I. Sur, H. Scherrer, and Z. Dashevsky, Phys. Rev. B **61**, 15965 (2005).
[9] Z. Bian, M. Zebarjadi, R. Singh, Y. Ezzahri, A. Shakouri, G. Zeng, J. H. Bahk, J. E. Bowers, J. M. O. Zide, and A. C. Gossard, Phys. Rev. B **76**, 205311 (2007).
[10] A. Ishida, Y. Sase, and H. Fujiyasu, Appl. Surf. Sci. **33**, 868 (1988).
[11] A. Ishida, S. Matsuura, M. Mizuno, and H. Fujiyasu, Appl. Phys. Lett. **51**, 478 (1987).
[12] A. Ishida, M. Veis, and Y. Inoue, Jpn. J. Appl. Phys., Part 2 **46**, L.281 (2007).
[13] S. Takaoka, T. Itoga, and K. Murase, Jpn. J. Appl. Phys., Part 1 **23**, 216 (1984).
[14] H. Beyer, A. Lambrecht, J. Nunus, H. Böttner, H. Griessmann, A. Heinrich, L. Schmitt, M. Blumers, F. Völklein, Proceedings of the 18th International Conference on Thermoelectrics, ICT'99, Baltimore, Maryland, 29 August–2 September, 1999 (unpublished), p. 687.